Cold Regions Science and Technology 104–105 (2014) 14–22

Contents lists available at ScienceDirect

Cold Regions Science and Technology

journal homepage: www.elsevier.com/locate/coldregions

A moving-pump model for water migration in unsaturated freezing soil

Jiazuo Zhou [a], Changfu Wei [a,*], Dongqing Li [b], Houzhen Wei [a]

[a] State Key Laboratory of Geomechanics and Geotechnical Engineering, Institute of Rock and Soil Mechanics, Chinese Academy of Sciences, Wuhan 430071, China
[b] State Key Laboratory of Frozen Soil Engineering, Cold and Arid Regions Environmental and Engineering Research Institute, Chinese Academy of Sciences, Lanzhou 730000, China

ARTICLE INFO

Article history:
Received 29 November 2013
Accepted 30 April 2014
Available online 9 May 2014

Keywords:
Unsaturated freezing soil
Water migration
Heat transfer
Moving-pump model
Numerical procedure

ABSTRACT

This paper presents a new approach for simulating the water migration in freezing soils, in which the pore water migration and heat transfer are characterized using an imaginary pump attached with a small imaginary reservoir. The pump moves with the freezing front as temperature decreases, sucks the liquid water from the unfrozen zone and then stores it in the frozen zone. The reservoir is used to gather the sucked water and store it in the form of pore ice through phase change. Explicit governing equations are developed for describing the water migration, crystallization and/or heat transfer in the soil, the pump and the reservoir. The proposed model is numerically implemented into a commercial code. Compared to the previous approaches used to simulate the soil freezing processes, application of the new approach avoids remeshing and recalculating the moving boundaries, and this feature can drastically simplify the numerical implementation of the theoretical model. The new approach is used to analyze the one-dimensional freezing process in soils. The simulated results are compared with the experimental data available in the literature and the simulations based on other approaches, showing that the new approach is capable of effectively simulating the freezing process of soils.

1. Introduction

Any freezing process in soil is accompanied by both heat and pore water transfers, and these processes occur in a coupled manner. During a freezing process, a temperature gradient forms in the soil, driving the heat to flow from the higher-temperature zone toward the lower-temperature zone and the pore water to migrate from the unfrozen zone to the frozen zone. The pore water migration driven by temperature can influence the heat conduction process due to the effect of convection and latent heat of phase change, while the heat conduction may induce phase change and in turn change the hydraulic conductivity of the soil (Harlan, 1973; O'Neill and Miller, 1985; Taylor and Luthin, 1978). In addition, both heat and mass transfer can change the physical and mechanical properties of the soil. In analyzing the problems related to soil freezing, it is crucial to properly characterize both heat and pore water transferring processes.

If a fully saturated soil with a sufficient water supply begins to freeze, the soil water will constantly migrate to the frozen zone from the unfrozen region due to the effect of cryosuction, resulting in an increase in the water content of the frozen zone, while the water content in the unfrozen zone remains practically unchanged. Therefore, in analyzing the freezing process of a fully saturated soil with a sufficient water supply, only the water increase in the frozen zone and consequently the total frost heave are of concern, and the problem can be solved by ignoring the effect of the water content variation and the skeletal deformation in the unfrozen zone (Xu and Deng, 1991; Zhou et al., 2011). In the freezing process of an unsaturated soil, however, the water migration is more complex, and this is the case especially for a closed system, i.e., the soil without a water supply. In this case, the water content increases in the frozen zone while decreases in the unfrozen zone. The problem is complicated by the movement of the interface between the frozen and the unfrozen zone with temperature.

To simulate the processes of heat and water transfer in unsaturated freezing soil, Chen et al. (1990) and Hu et al. (1992) developed the governing equations of water migration in the frozen and unfrozen zones, respectively. It is remarkable, however, that in applying these equations, a boundary condition has to be introduced to ensure the flow continuity between the frozen and unfrozen zones. As such, when the interface moves with the freezing front, the boundary condition of these two equations also vary with temperature. Hence, if a finite element or finite difference procedure is adopted in the simulation, it is necessary to remesh and recalculate the moving boundary after each time step. In addition to this complexity, the high nonlinearity of the governing equations and the coupling of heat and water transfer make the simulation procedure rather difficult (Black, 1995a; Chen et al., 1990; Hu et al., 1992; O'Neill and Miller, 1985; Taylor and Luthin, 1978; Zhou and Zhou, 2010).

In this paper a new approach is presented to simulating the one-dimensional pore water migration in freezing unsaturated soils. In this approach, the frozen fringe can be envisioned as a moving pump,

* Corresponding author. Tel.: +86 27 87197239; fax: +86 27 8719 8346.
E-mail address: cfwei@whrsm.ac.cn (C. Wei).

http://dx.doi.org/10.1016/j.coldregions.2014.04.006

which sucks pore water from the unfrozen zone and store it as pore ice through phase transition in the frozen zone. To characterize the crystallization of the sucked pore water, a small imaginary reservoir is introduced, which is attached to the moving pump and used for collecting the sucked pore water and related phase transition. During the soil freezing, the pump and the reservoir simultaneously move as the temperature decreases. Governing equations are then developed for the water migration and heat transfer as well as phase transition in the pump and/or in the reservoir. As such, in simulating the soil freezing process, it is not necessary to change the boundary conditions of the solution domain, and the theoretical model can be readily implemented into a commercial code without complex programming.

2. Theory

2.1. The driving force for water migration in freezing soil

In a frozen soil, a certain amount of unfrozen water exists in the vicinity between the surfaces of soil grains and ice grains due to the premelting effect (Wettlaufer and Worster, 1995; Wettlaufer et al., 1996; Xu et al., 1993). At equilibrium, the pressures of the unfrozen pore water and the pore ice can be related to each other through the generalized Clapeyron equation (Black, 1995b), i.e.,

$$\mathrm{d}u_w = \frac{\rho_w}{\rho_i}\mathrm{d}u_i + \frac{\Delta H \rho_w}{T_0}\mathrm{d}T \tag{1}$$

where u_w and u_i are the pressures of unfrozen pore water and pore ice, respectively; ρ_w and ρ_i are the densities of pore water and pore ice, respectively; T_0 (K), T(°C) and ΔH are the freezing point of bulk water, the current temperature and the latent heat of fusion, respectively. Without overburden loading, u_i remains practically unchanged, while u_w decreases linearly with temperature according to Eq. (1).

Strictly, the generalized Clapeyron equation is valid only in the case that unfrozen pore water and pore ice coexist in equilibrium. In any transient process, however, this equilibrium condition cannot be strictly achieved. In the following, it is assumed that the temperature change and the water migration are slow enough compared to the phase change, so that Eq. (1) is valid under the transient condition. Eq. (1) implies that, if ice pressure gradient is neglected, a temperature gradient can induce pore water pressure gradient, driving the pore water to migrate from the higher temperature zone to the lower temperature zone.

Harlan (1973) assumed that the potential of pore water in the frozen soil equals to that in the unsaturated soil with the same liquid water content. This assumption has been validated using the soil–water characteristic curve (SWCC) and the soil freezing characteristic curve (SFCC) of the soil under partially saturated and frozen conditions, respectively (Azmatch et al., 2012; Liu et al., 2011; Spaans and Baker, 1996). Indeed, according to the generalized Clapeyron equation, one can easily see that, if the ice pressure is constant and capillary hysteresis is excluded, there is a one-to-one correspondence between unfrozen water content and temperature in the frozen soil. Hence, both the pore water pressure and the temperature in the frozen soil (with undercooling pore water) can be expressed as a function of unfrozen water content only. Based on the above discussions, it is suggested that, if the ice pressure remains constant and its gradient is neglected, the driving force of water migration in the frozen soil can be expressed as the gradient of unfrozen water content.

2.2. Governing for water migration and heat transfer

Based on the above discussions, if the gradient of ice pressure is negligible, the seepage velocity can generally be expressed as the diffusivity multiplying the gradient of unfrozen water content (Shao et al., 2006). Recalling the assumption that the heat conduction and the water migration are slow enough compared to the phase change (between liquid water and ice), one obtains the governing equation for water migration in frozen soils, which in a form similar to the Richards Equation (Richards, 1931; Taylor and Luthin, 1978):

$$\frac{\partial}{\partial t}\left(\theta_u + \frac{\rho_i}{\rho_w}\theta_i\right) = \frac{\partial}{\partial x}\left(D\frac{\partial \theta_u}{\partial x}\right) \tag{2}$$

where t and x represent the elapsing time and the spatial coordinate, respectively; D is the water diffusivity; θ_u is the specific unfrozen (or liquid) water content; θ_i is the specific ice content. The term in the bracket of the left-hand side is equal to the total specific water content (including both liquid water and ice). Hereinafter both ρ_w and ρ_i are assumed to be constant. Eq. (2) implies that any change in the total specific water content of the frozen soil is solely due to the transfer of unfrozen water.

In general, the migrating process of pore water in a frozen soil is slow, and thus its effect on heat convection is negligible. Hence, one obtains the heat conduction equation as (Taylor and Luthin, 1978):

$$C\frac{\partial T}{\partial t} = \frac{\partial}{\partial x}\left(\lambda\frac{\partial T}{\partial x}\right) + L\rho_i\frac{\partial \theta_i}{\partial t} \tag{3}$$

where C is the volumetric heat capacity, λ is the thermal conductivity of the soil, and L is the latent heat of fusion (per unit mass of water).

In a freezing soil subjected to a temperature gradient, two processes associated with crystallization in the pores may simultaneously occur. Indeed, as the temperature decreases, part of the liquid water at the site may change into ice, while a certain amount of liquid water is sucked from the higher-temperature zone into the frozen zone where it crystallizes. Correspondently, the variation of θ_i (Eq. (3)) can be additively decomposed into two components (Penner and Ueda, 1978; Zhou et al., 2011): one is due to the crystallization of the liquid pore water at the site (denoted as $\mathrm{d}\theta_1$), and the other is due to the crystallization of the sucked liquid water (i.e., the water transferred from other places), which is denoted as $\mathrm{d}\theta_2$. Then, the variation of the specific ice content can be expressed as

$$\mathrm{d}\theta_i = \mathrm{d}\theta_1 + \mathrm{d}\theta_2 \tag{4}$$

where

$$\mathrm{d}\theta_1 = -\frac{\rho_w}{\rho_i}\mathrm{d}\theta_{in} \tag{5}$$

and

$$\frac{\partial \theta_2}{\partial t} = \frac{\rho_w}{\rho_i}q \tag{6}$$

where θ_{in} is the specific content of the liquid water that changes into pore ice at the site, and q is the changing rate of the specific content of the liquid water sucked from the higher-temperature zone. Eq. (6) implies that all the liquid water sucked from the higher-temperature zone changes into pore ice.

Substituting Eqs. (4)–(6) into Eq. (3), one obtains

$$C_e\frac{\partial T}{\partial t} = \frac{\partial}{\partial x}\left(\lambda\frac{\partial T}{\partial x}\right) + L\rho_w q \tag{7}$$

where C_e is the equivalent volumetric heat capacity, defined by

$$C_e = C + L\rho_w\frac{\partial \theta_{in}}{\partial T} \tag{8}$$

Clearly, C_e includes a component related to the latent heat that is released by the phase change at the site (Bonacina et al., 1973).

2.3. A moving-pump model

2.3.1. Conception of the model

In a soil freezing under certain temperature gradient, a frozen fringe of a certain thickness usually develops in the vicinity of the freezing front (Miller, 1972). In the frozen fringe, unfrozen pore water and pore ice coexist; on the cooler side of the fringe, there exists a frozen zone where ice lenses and pore ice exist (sometimes including a small amount of strongly adsorbed water); on the warmer side of the fringe, there is an unfrozen zone where no pore ice can exist. During a freezing process, the frozen fringe moves as temperature decreases in the same direction as the temperature gradient. As temperature decreases, two processes occur in the freezing soil, i.e., the liquid pore water crystallizes locally at the site, while some amount of liquid water migrates into the fringe from the unfrozen zone and then crystallizes in the frozen zone.

To characterize these processes, we assume that the frozen fringe is a “thin” transition zone, located between the frozen zone and the unfrozen zone. If the actual thermodynamic processes occurring in this zone are not of concern, the frozen fringe can be envisioned as a small pump (Fig. 1), which moves as temperature varies. The role of this imaginary pump is to suck the liquid water from the unfrozen zone and then to store it in the frozen zone where the sucked water crystallizes. To characterize the crystallization of the sucked liquid water, we assume that a small reservoir is attached to the cooler boundary of the frozen fringe. The role of the imaginary reservoir is to collect the sucked water and to provide a room for the collected water to crystallize. As such, during the freezing process, the pump (i.e., the frozen fringe) and the water gathering reservoir simultaneously moves as temperature changes, and some amount of liquid water is sucked into the reservoir where it crystallizes.

As schematically illustrated in Fig. 1, the pump is defined by a temperature transition interval, i.e., $[-T_t,T_t]$, where T_t is a small positive number. Although not necessarily defined explicitly, the temperature transition interval is supposed to cover the whole range of temperature variation in the frozen fringe. The water gathering reservoir is defined by temperature interval $[-T_t-2T_d, -T_t]$, where T_d is a small positive number, and $2T_d$ equals the temperature difference between the two ends of the reservoir. Under a specified temperature gradient, these temperature intervals can also be transformed into the spatial domain. Remarkably, however, it is not necessary to perform such transformation explicitly in the following derivations.

2.3.2. Model description

According to the conceptual model described in Section 2.3.1, the process of water migrating from the unfrozen zone into the frozen zone can be characterized using an imaginary pump, which sucks liquid water from the unfrozen zone and stores the water intake in the frozen zone. To realize this, one can decompose Eq. (2) into two equations. The first equation is used to describe the water migration in the unfrozen zone, and can be expressed as

$$\frac{\partial\theta_u}{\partial t}=\frac{\partial}{\partial x}\left(D\frac{\partial\theta_u}{\partial x}\right)-q \tag{9}$$

and the second equation describes the water gathering in the imaginary reservoir in the form of ice

$$\frac{\partial\theta_f}{\partial t}=q \tag{10}$$

where $\theta_f=\rho_i\theta_i/\rho_w$ and q has been defined in Eq. (6) which is related to the “power of the pump”. Here, it is implicitly assumed that the time scale of water crystallization is much shorter than that of water migration, so that once the pore water is sucked into the reservoir, it immediately crystallizes. Clearly, the total specific water content θ is equal to the sum of θ_u and θ_f.

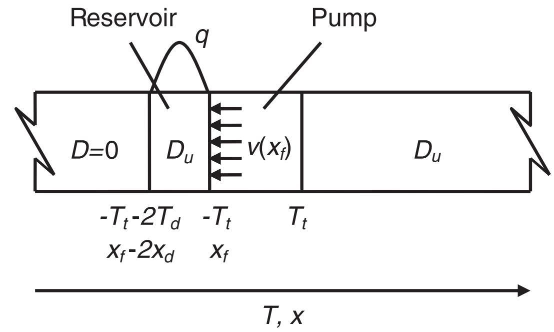

Fig. 1. Schematic diagram of moving-pump and reservoir.

Because the water migrating process ceases in the frozen zone, one can assume that

$$D=\begin{cases}D_u & T\geq -T_t-2T_d\\ 0 & T<-T_t-2T_d\end{cases}. \tag{11}$$

With the temperature gradient being given, D can also be defined in the spatial domain, namely,

$$D=\begin{cases}D_u & x\geq x_f-2x_d\\ 0 & x<x_f-2x_d\end{cases}. \tag{12}$$

Here, x_f is the spatial coordinate of the point with temperature $(-T_t)$, while (x_f-2x_d) represents the spatial coordinate at the end of the water gathering reservoir with $(-T_t-2T_d)$. Function D in Eq. (11) implies that the water migrating process stops when the liquid water enters into the frozen zone.

With these equations, the water migrating process can be envisioned as the movement of a pump with the isotherm, which sucks the liquid water from the unfrozen zone into the reservoir where the sucked water crystallizes as temperature decreases.

To calculate q, we consider the water gathering process in the reservoir. Under the 1-D condition and a specified temperature gradient, the reservoir can be represented by either the spatial interval $[x_f-2x_d, x_f]$ or the temperature transition interval $[-T_t-2T_d, -T_t]$, as schematically shown in Fig. 1.

The flow velocity of pore water from the unfrozen zone to the frozen zone is given by:

$$v\left(x_f\right)=D\frac{\mathrm{d}\theta_u}{\mathrm{d}x}\Big|_{x=x_f}. \tag{13}$$

This equation can be equivalently written as

$$v\left(x_f\right)=\int_{-\infty}^{+\infty}D\frac{\partial\theta_u}{\partial x}\delta(T+T_t)\mathrm{d}T \tag{14}$$

where $\delta(T+T_t)$ is the Dirac function which equals infinity in the case of $T=-T_t$ and equals to 0 in the case of $T\neq -T_t$. The integral of $\delta(T+T_t)$ from $-\infty$ to ∞ equals 1. The Dirac function $\delta(T+T_t)$ can be approximately represented by a bell-shaped pulse function $\Delta(T+T_t+T_d, T_d)$, which equals to 0 in the case of $T<-T_t-2T_d$ and $T>-T_t$, satisfying

$$\int_{-\infty}^{\infty}\Delta(T+T_t+T_d,T_d)\mathrm{d}T=\int_{-T_t-2T_d}^{-T_t}\Delta(T+T_t+T_d,T_d)\mathrm{d}T=1. \tag{15}$$

Clearly, when T_d assumes an infinitesimal value, $\Delta(T+T_t+T_d, T_d)$ approaches to $\delta(T+T_t)$.

Noting that T is a function of x, one can recast Eq. (14) into

$$v\left(x_f\right)\approx\int_{-\infty}^{+\infty}D\frac{\partial\theta_u}{\partial x}\frac{\partial T}{\partial x}\Delta(T+T_t+T_d,T_d)\mathrm{d}x \\ =\int_{x_f-2x_d}^{x_f}D\frac{\partial\theta_u}{\partial x}\frac{\partial T}{\partial x}\Delta(T+T_t+T_d,T_d)\mathrm{d}x. \tag{16}$$

According to its very physical meaning (cf. Eq. (6)), q is the derivative of $v(x_f)$ with $2x_d$ (i.e., the volume of the reservoir), and one obtains

$$q=D\frac{\partial\theta_u}{\partial x}\frac{\partial T}{\partial x}\Delta(T+T_t+T_d,T_d). \tag{17}$$

In deriving Eq. (17), it is assumed that the gradient of ice pressure is negligible (see Sections 2.1 and 2.2). In reality, however, an ice pressure gradient may exist in the frozen soil (Gilpin, 1980; O'Neill and Miller, 1985). To account for the effect of the ice pressure gradient, one can prove that (see the Appendix A)

$$\frac{\partial\theta_u}{\partial x}=f\frac{\partial\theta_u}{\partial T} \tag{18}$$

where f is given by

$$f=\frac{T_0}{\rho_i\Delta H}\frac{\partial u_i}{\partial x}+\frac{\partial T}{\partial x}. \tag{19}$$

In general, the direction of ice pressure gradient is opposite to that of temperature gradient, i.e., the existence of the ice pressure gradient hinders the water flowing into the frozen zone. Eq. (19) implies that f is a function of both the ice pressure gradient and the temperature gradient. The ice pressure gradient is associated with discrete ice lens formation and temperature gradient. Because the ice lens formation is not of concern in this paper, one can simply assume that the ice pressure gradient depends upon the temperature gradient only. Therefore, coefficient f can be viewed as a function of the temperature gradient, which has yet to be determined.

After substituting Eq. (18) into Eq. (17), it immediately follows that

$$q=Df\frac{\partial\theta_u}{\partial T}\frac{\partial T}{\partial x}\Delta(T+T_t+T_d,T_d). \tag{20}$$

Similarly, in the spatial domain, one has

$$q=Df\frac{\partial\theta_u}{\partial T}\Delta\left(x-x_f+x_d,x_d\right). \tag{21}$$

In the frozen soil, the unfrozen water content can be expressed as a function of temperature, i.e.,

$$\theta_u=w(T). \tag{22}$$

Derivative $\partial\theta_u/\partial T$ can be considered as a function of θ_u, that is, one can write

$$\frac{\partial\theta_u}{\partial T}=w'\left[w^{-1}(\theta_u)\right] \tag{23}$$

where w' and w^{-1} are the derivative and inverse functions of T, respectively.

As derived above, the reservoir can be viewed as the engine of the pump, and the power of the engine is described by Eq. (21). It is remarkable that we assign diffusivity D_u to the reservoir through Eqs. (11) and (12) simply because the diffusivity accounts for the power of the engine, and no water migrating process can actually occur in the reservoir.

2.3.3. Material properties

The theoretical model developed above includes two material parameters yet to be determined, i.e., volumetric heat capacity C and thermal conductivity λ. In general, these parameters depends upon the volume fractions of individual bulk phases, which include the liquid pore water, pore ice, solid grains and/or pore gas. In the following, it is assumed that the volume fractions of individual bulk phases vary only slightly in both frozen zone and unfrozen zone so that C and λ are practically constant in both frozen and unfrozen zones. The volumetric heat capacity and thermal conductivity are denoted as C_f and λ_f, respectively, for the frozen zone and C_u and λ_u, respectively, for the unfrozen zone. To determine the material parameters for the freezing fringe, one can introduce a piecewise function $H(T,\ T_t)$, which is defined by (Zimmerman, 2007)

$$H(T,T_t)=\begin{cases}0 & T<-T_t\\ \dfrac{3T}{4T_t}-\dfrac{T^3}{4T_t{}^3}+\dfrac{1}{2} & -T_t\le T\le T_t\\ 1 & T>T_t\end{cases}. \tag{24}$$

It can be proved that the derivative of $H(T,T_t)$ is a bell-shaped pulse function, whose integral over the whole real number field equals 1 (cf. Eq. (15)). Hence, with Eq. (24), one can define function $\Delta(T,\ T_t)$ as

$$\Delta(T,T_t)=\frac{dH(T,T_t)}{dT}. \tag{25}$$

Functions H and Δ are schematically shown in Figs. 2 and 3, respectively.

By using function $H(T,\ T_t)$, the thermal conductivity and the volumetric heat capacity for the freezing fringe can be analytically expressed as

$$\lambda=\lambda_f+\left(\lambda_u-\lambda_f\right)H(T,T_t) \tag{26}$$

$$C=C_f+\left(C_u-C_f\right)H(T,T_t). \tag{27}$$

Eqs. (26) and (27) imply that C and λ in the freezing fringe vary with the temperature, in a sharp contrast to those in the frozen and unfrozen zones.

3. Numerical examples

The proposed model has been implemented into a commercial computer code, Comsol Multiphysics. To illustrate its capability, the

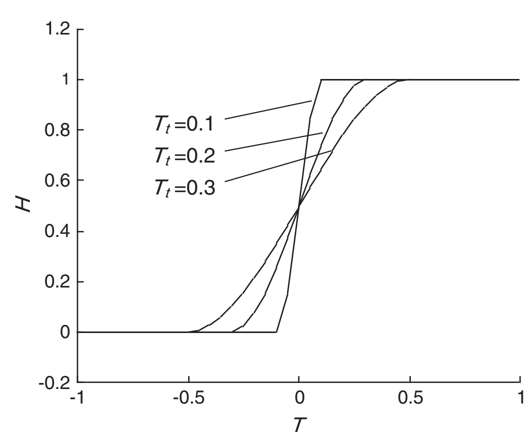

Fig. 2. Schematic of function *H*.

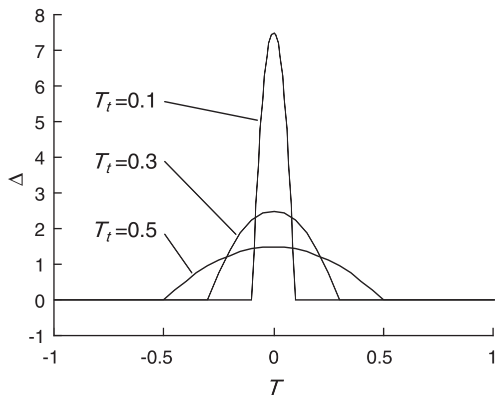

Fig. 3. Schematic of function Δ.

proposed model is used to analyze two examples related to the one-dimensional water migration and heat transfer in freezing soils.

3.1. Example 1

Hu et al. (1992) performed a one-dimensional (vertical) freezing experiment, during which a partially saturated soil column was frozen from the top to the bottom without an external water supply. The tested material was a loamy soil. The soil sample is 13.68 cm high, with a dry density of 1.5 g/cm^3 and an initial saturation degree of 49.68% (corresponding to an initial water content of 0.2208). During the experiment, the side wall of the sample was adiabatic, and the temperatures on the top and the bottom of the sample were controlled by circulating a coolant around the sample. The relationship between unfrozen water content and temperature is shown in Fig. 4, and can be expressed as

$$\theta_u = \begin{cases} 0.89T + 0.4336, -0.37 \le T \le 0 \\ 0.0045(T+0.4) + 0.0776, T < -0.37 \end{cases}. \quad (28)$$

It can be seen that, when the temperature decreases from the real freezing point T_f to −0.37 °C, the unfrozen water content decreases drastically from the initial volumetric water content at the freezing front (denoted as θ_r) to 0.1043, and in a sharp contrast, when the temperature is lower than −0.37 °C, the unfrozen water content decreases only slightly with temperature. Hence, it is proposed herein that θ_{in} can be expressed as

$$\theta_{in} = 0.1043 + (\theta_r - 0.1043)H(T, T_t) \quad (29)$$

which implies that θ_{in} is equal to 0.1043, in the frozen zone ($T < -T_t$), and θ_r, in the unfrozen zone ($T > T_t$).

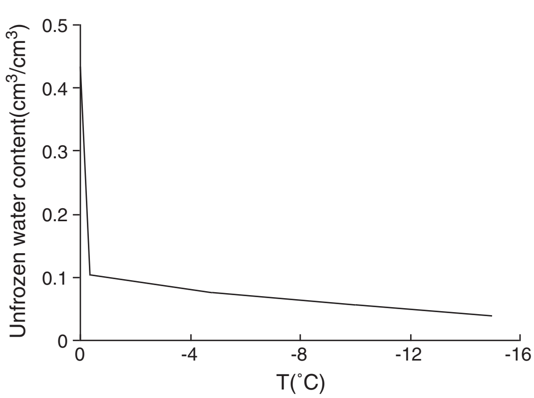

Fig. 4. The relationship between unfrozen water and temperature (after Hu et al. (1992)).

Neglecting the effect of the phase change at the temperature lowering than −0.37 °C, one can obtain the latent heat due to the phase change at the site as

$$\int_{-T_t}^{T_t} L\rho_w \frac{\partial \theta_{in}}{\partial T} \mathrm{d}T = \int_{-0.37}^{\theta_r} L\rho_w \frac{\partial \theta_u}{\partial T} \mathrm{d}T. \quad (30)$$

Eq. (30) transforms the real temperature interval for the phase change to the temperature transition interval [$-T_t$, T_t] based on the equivalence of releasing latent heat. Then the equivalent volumetric heat capacity (Eq. (8)) is

$$C_e = C + L\rho_w(\theta_r - 0.1043)\Delta(T, T_t). \quad (31)$$

Although the unfrozen water content may vary in the moving frozen zone, its variation is expected to be very small in the zone [$-T_t$, T_t] so that$\theta_r \approx \theta_u$. Consequently the Eq. (31) can be approximated by

$$C_e = C + L\rho_w(\theta_u - 0.1043)\Delta(T, T_t). \quad (32)$$

The thermal conductivities and volumetric heat capacity are not available for the tested material. Here, the typical values of these parameters for a silty soil (Xu et al., 2010) are taken as references, and it is assumed that, λ_f = 1.58 W/(m·K), λ_u = 1.13 W/(m·K), C_f = 2820 kJ/(m^3·K) and C_u = 2360 kJ/(m^3·K).

According to Eqs. (23) and (28)

$$\frac{\partial \theta_u}{\partial T} = \begin{cases} 0.89 & \theta_u \ge 0.1043 \\ 0.0045 & \theta_u < 0.1043 \end{cases}. \quad (33)$$

The diffusivity (cm^2/min) of unfrozen soil depends upon the degree of liquid water saturation, and it is assumed as (Hu et al., 1992)

$$D_u = 2.03S^{7.35} \quad (34)$$

where S is the degree of saturation of the liquid water, which equals the specific water content θ divided by the porosity n (n = 0.4444). Function f in Eq. (18) is assumed as

$$f = \frac{1}{10}\frac{\partial T}{\partial x}. \quad (35)$$

The initial temperature distribution and the boundary condition are shown in Tables 1 and 2. The initial specific water content is 0.2208, and hence the initial values of θ_u and θ_f are 0.2208 and 0, respectively. All the boundary conditions for θ_u and θ_f are of Neumann's type. Other parameters in the moving-pump model for this example are T_t(0.3 °C) and T_d(0.3 °C).

Fig. 5 illustrates the simulations for θ_u and θ_f distributions at different moments. It can be seen that during the freezing process, the volumetric water content decreases in the unfrozen zone and increases in the frozen zone. This phenomenon can be easily understood, because during the freezing process no external water was supplied to the soil column and the liquid water was "sucked" from the unfrozen zone and stored in the frozen zone. The simulated and measured results of the total specific water content distribution at 47.2 h are compared in Fig. 6. Figs. 7 and 8 show the simulated and measured movement of freezing front (approximately the isotherm of 0 °C) and temperature distribution, respectively. Hu et al.'s (1992) simulation is also given for comparison in these figures. It can be seen that both the simulated results agree reasonably well with the experimental result. Remarkably, however, the simulation procedure proposed here is much simpler than that followed by Hu et al. (1992), which was based on the finite differential method, in that remeshing and recalculating the moving boundary is not required in the new approach.

As discussed above, there are two sources of latent heat, one of which originates from the phase change at the site and the other

Table 1
Initial temperature distribution (After Hu et al. (1992)).

Depth (cm)	0.00	1.52	3.04	4.56	6.08	7.60	9.12	10.64	12.16	13.68
T (°C)	11.42	15.48	16.36	16.75	16.84	16.89	16.84	16.90	16.79	16.41

originates from the phase change of the water migrating from the unfrozen zone. Consequently, the following three cases need to be addressed, including: 1) both the two kinds of phase change are involved in, 2) only the crystallization of pore water at site is considered, and 3) none of the two kinds of phase change is considered. The simulated results in Figs. 6–8 are obtained for the first case. The variation of temperature with time at the depths of 4 cm (frozen) and 10 cm (unfrozen) are presented in Fig. 9 for all the three cases. It can be seen that the temperature changes in case 1 and case 2 are very close to each other, and the temperature change curve in case 3 is significantly different from the other two curves. In addition, the temperature in all the three situations tends to be coincident as time elapses. This is because the water content in the unfrozen zone becomes very low after a long time of water and heat transfer, and consequently the diffusivity of unfrozen zone becomes very low so that there is not sufficient liquid water to migrate to the frozen zone and the released latent heat of phase change is very small.

3.2. Example 2

In Example 1, the temperature and the specific water content are solved in a fully coupled manner. Fig. 9 illustrates that the results of Case 1 (involving both at-site phase change and water migration) and Case 2 (involving at-site phase change only) are quite similar to each other, implying the effect of water migration on the heat transfer is insignificant. Hence, it is tempting to solve the problem in an uncoupled way. To this end, we try to first determine the temperature field and then, with the obtained temperature field, to determine the volumetric water content. From Fig. 8, one can see that when the temperature is lower than 0, it varies linearly with the depth. Hence, the temperature gradient is approximately equal to the difference between 0 °C and the colder boundary temperature divided by the distance between 0 °C and the colder boundary. With the obtained temperature data, one can determine the moving rate of the pump and the value of q, and finally obtain the volumetric water content.

Jame and Norum (1976) reported experimental results on a silica sand, which were later analyzed by Taylor and Luthin (1978) based on the finite differential method. In the following, we adopt the uncoupled procedure introduced above to solve the problem. In Jame and Norum's experiment, the dry density of the tested soil is 1.35 g/cm^3, with an initial mass water content of 0.205 g/g. Based on the experimental data, we obtain the equivalent volumetric heat capacity as

$$C_e = C + (0.2768 - 0.005)L\rho_w\Delta(T, T_t). \quad (36)$$

The initial temperature and boundary temperature are the same as those in Taylor and Luthin (1978). The thermal conductivities of the soil in the frozen zone and unfrozen zone are unavailable, and they are assumed to be 2.6 W/(m·K) and 1.6 W/(m·K), respectively. The volumetric heat capacities of the soil in the frozen zone and the unfrozen zone are assumed to equal 1500 kJ/(m^3·K) and 1820 kJ/(m^3·K), respectively. In calculation, $T_t = 0.25$ °C, respectively.

Comparison of the measured and simulated temperature distributions are shown in Fig. 10, from which it can be seen that the simulated temperature agrees very well with the measured data. The position of 0 °C is equal to the length of frozen soil and the calculated value (denoted as "+") can be determined as $x_f = 14.94\,e^{0.00381t} - 13.57\,e^{-0.07695t}$ using the trial-and-error procedure (Fig. 11). Because the temperature distribution in frozen soil is practically linear, the temperature gradient is determined by dividing the difference between colder boundary temperature and 0 °C by the length of frozen soil, and the results are also presented in Fig. 11.

According to the measurement on the variation of unfrozen water content with temperature (Taylor and Luthin, 1978), the derivative of unfrozen water content with respect to temperature can be expressed as

$$\frac{\partial\theta_u}{\partial T} = \begin{cases} 0.76, \theta_u \geq 0.07 \\ 0.713 \times \ln 10 \times \left(\frac{\theta_u}{0.713}\right), (\theta_u < 0.07) \end{cases}. \quad (37)$$

Table 2
Temperature variations on the boundaries (After Hu et al. (1992)).

Time (min)	0	34	55	86	367	401	445
Top (°C)	11.42	0.98	−0.68	−2.16	−1.34	−2.29	−2.85
Bottom (°C)	16.41	15.63	6.78	4.65	4.83	4.45	4.01
Time (min)	528	767	1374	1595	1837	2177	2830
Top (°C)	−3.38	−4.27	−4.86	−4.83	−4.86	−4.88	−4.86
Bottom (°C)	3.93	3.8	3.59	3.62	3.62	3.59	3.67

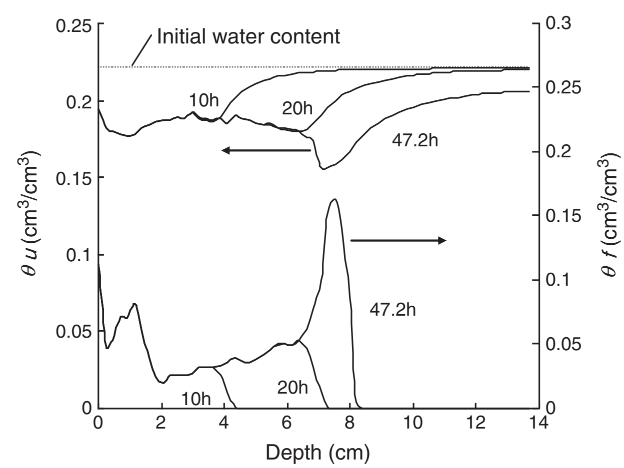

Fig. 5. Distributions of θ_u and θ_f at different moments.

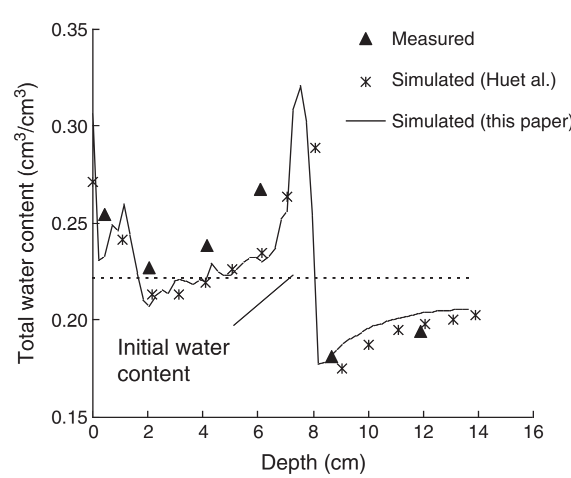

Fig. 6. Comparison of the measured and simulated distributions of water content at 47.2 h.

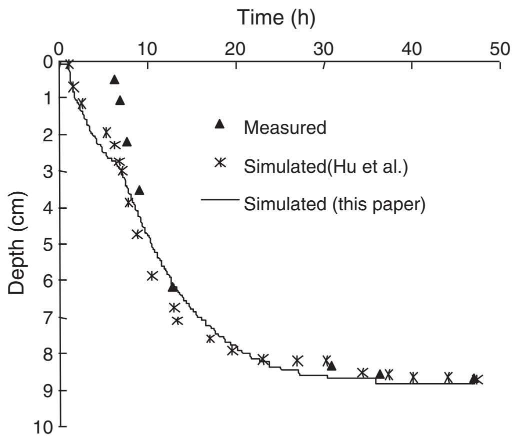

Fig. 7. Comparison of measured and simulated 0 °C isotherms.

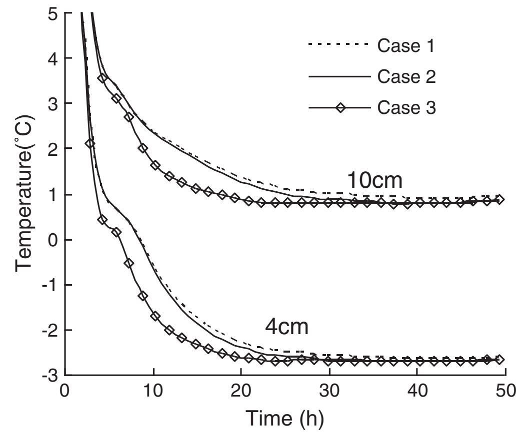

Fig. 9. Variations of temperature with time.

The diffusivity (cm^2/h) of the soil is (Jame and Norum, 1976)

$$D = 10^{7.03(\theta_u - 0.1) - 3.25} (\theta_u \geq 0.1) \\ = 10^{15.14(\theta_u - 0.01) - 4.55} (\theta_u < 0.1). \tag{38}$$

Parameter x_d in Eq. (21) assumes a value of 0.7 cm in the simulation.

As to coefficient f, we consider the following two cases. In the first case, it is assumed that

$$f = \frac{1}{100} \frac{\partial T}{\partial x}. \tag{39}$$

The simulated water content distribution is presented in Fig. 12 (denoted as "simulation A"), showing that the water content in the zone near the left boundary is overestimated by the simulation A. This is because the temperature gradient within the first 10 h is high (Fig. 11), so that f becomes very large, resulting in a greater water migrating velocity (into the frozen zone).

To reduce the value of f in the early stage of freezing, we assume another form of f, which is expressed as

$$f = \begin{cases} \frac{dT}{dx}, & \frac{dT}{dx} \leq 0.2 \\ 0.2 + 0.002 \times \left(\frac{dT}{dx} - 0.2 \right), & \frac{dT}{dx} > 0.2. \end{cases} \tag{40}$$

The simulation of water content distribution is presented in Fig. 12 (denoted as "simulation B"). It can be seen that the simulated result is much closer to the measurement, compared to simulation A. In Taylor and Luthin's simulation, a resistance factor was adopted for the diffusivity of the soil in the frozen zone, and this factor ranges from 100 to 1000. Their simulated results are also shown in Fig. 12. From the comparisons in Fig. 12, the capability of the moving-pump model is clearly demonstrated.

4. Conclusions

In this paper a simple model for simulating the soil freezing process is developed, in which the water and heat transferring processes are characterized by using an imaginary pump attached with a small reservoir. The role of the pump is to suck the liquid water from the unfrozen zone and then to store it in the frozen zone, whereas the role of the imaginary reservoir is to gather the sucked water and store it in the form of pore ice through phase changes. As such, during the freezing process, the pump and the reservoir move simultaneously as temperature changes. Compared to other models used to simulate freezing processes, application of the new model avoids remeshing and recalculating the moving boundaries, which makes the numerical implementation of the model much simpler. Two numerical examples are presented. The simulated results are compared with experimental data and those previous simulations based on other approaches, showing that the proposed model is capable of effectively simulating the freezing process of soils.

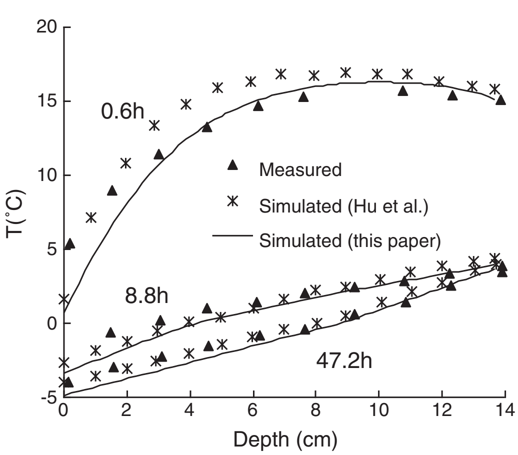

Fig. 8. Comparison of measured and simulated temperatures.

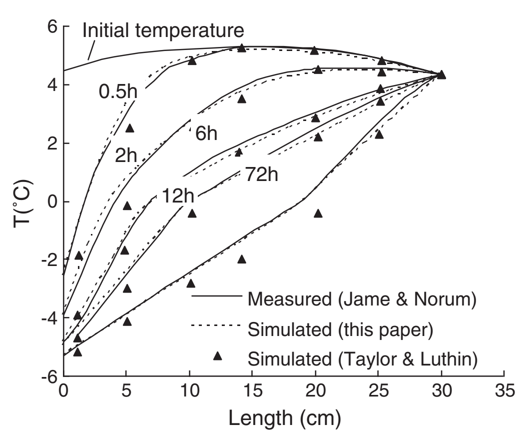

Fig. 10. Comparison of measured and simulated temperatures.

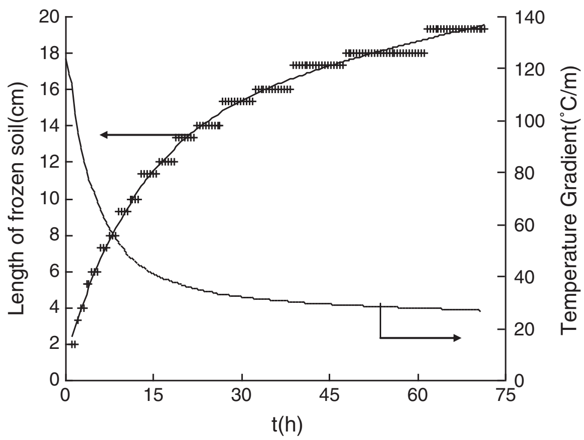

Fig. 11. Variations of the length of frozen soil and the temperature gradient.

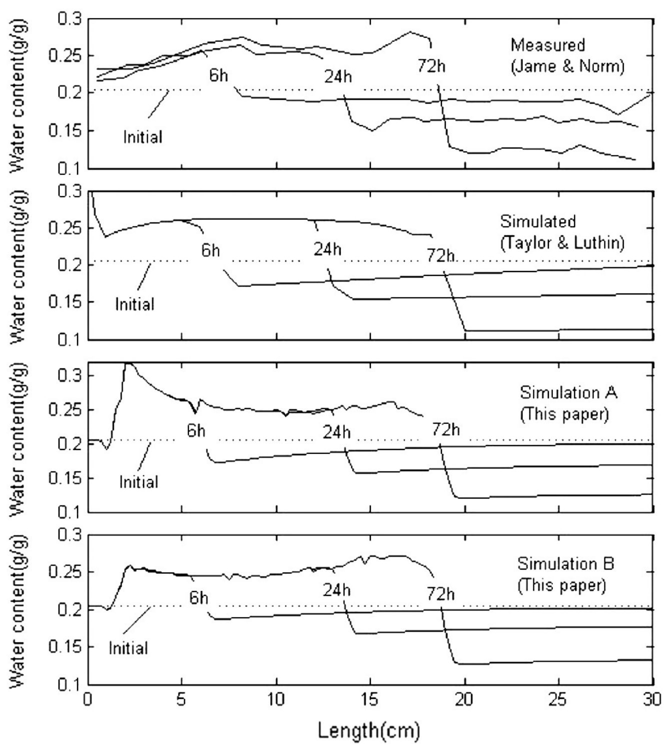

Fig. 12. Comparison of the experimental and simulated water distributions.

Acknowledgments

This research was funded by one of the National Basic Research Programs of China under grant #2012CB026102, and the National Science Foundation of China (NSFC) under grants #51239010 and #41102199.

Appendix A

The water pressure in a frozen soil is a function of the unfrozen water content (Azmatch et al., 2012; Liu et al., 2011; Spaans and Baker, 1996), and thus Eq. (1) can be expressed as

$$g(\theta_u)\mathrm{d}\theta_u = \frac{\rho_w}{\rho_i}\mathrm{d}u_i + \frac{\Delta H\rho_w}{T_0}\mathrm{d}T \tag{A1}$$

where $g(\theta_u)$ is a function of the unfrozen water content and determined by the experiment under the condition of $\mathrm{d}u_i = 0$. Hence, one can obtain

$$g(\theta_u) = \frac{\Delta H\rho_w}{T_0}\frac{\mathrm{d}T}{\mathrm{d}\theta_u} \tag{A2}$$

Substituting Eq. (A2) into Eq. (A1) yields

$$\mathrm{d}\theta_u = \frac{\mathrm{d}\theta_u}{\mathrm{d}T}\left(\frac{T_0}{\rho_i\Delta H}\mathrm{d}u_i + \mathrm{d}T\right) \tag{A3}$$

or

$$\frac{\partial\theta_u}{\partial x} = \frac{\partial\theta_u}{\partial T}\left(\frac{T_0}{\rho_i\Delta H}\frac{\partial u_i}{\partial x} + \frac{\partial T}{\partial x}\right) \tag{A4}$$

where $\partial\theta_u/\partial T$ is determined from the experiment under the condition of $\mathrm{d}u_i = 0$.

Appendix B. Supplementary data

Supplementary data to this article can be found online at http://dx.doi.org/10.1016/j.coldregions.2014.04.006.

References

Azmatch, T.F., Sego, D.S., Arenson, L.U., et al., 2012. Using soil freezing characteristic curve to estimate the hydraulic conductivity function of partially frozen soils. Cold Reg. Sci. Technol. 83–84, 103–109.
Black, P.B., 1995a. Rigid Ice Model of Secondary Frost Heave. Cold Regions Research & Engineering Laboratory, US Army Corps of Engineers.
Black, P.B., 1995b. Applications of the Clapeyron Equation to Water and Ice in Porous Media. Cold Regions Research & Engineering Laboratory, US Army Corps of Engineers.
Bonacina, C., Comini, G., Fasano, A., et al., 1973. Numerical solution of phase-change problems. Int. J. Heat Mass Transf. 16 (26), 1825–1832.
Chen, X., An, W., Ma, W., et al., 1990. Interaction among temperature, moisture and stress fields in frozen soil. Lanzhou University Press, Lanzhou, China pp. 113–138 (in Chinese).
Gilpin, R.R., 1980. A model for the prediction of ice lensing and frost heave in soils. Water Resour. Res. 16 (5), 918–930.
Harlan, R.L., 1973. Analysis of coupled heat-fluid transport in partially frozen soil. Water Resour. Res. 9 (5), 1314–1323.
Hu, H., Yang, S., Lei, Z., 1992. A numerical simulation for heat and moisture transfer during soil freezing. J. Hydraul. Eng. 7, 1–8 (in Chinese with English abstract).
Jame, Y.W., Norum, D.I., 1976. Heat and mass transfer in freezing unsaturated soil in a closed system. Proceedings, 2nd Conference on Soil Water Problems in Cold Regions, Edmonton, Alberta, Canada.
Liu, Z., Zhang, B., Yu, X., et al., 2011. A new freezing method for soil water characteristic curve measurement. Proceedings, Transportation Research Board 90th Annual Meeting, Washington, DC, USA.
Miller, R.D., 1972. Freezing and heaving of saturated and unsaturated soils. Highw. Res. Rec. 393, 1–11.
O'Neill, K., Miller, R.D., 1985. Exploration of a rigid ice model of frost heave. Water Resour. Res. 21 (3), 281–296.
Penner, E., Ueda, T., 1978. A soil frost-susceptibility test and a basis for interpreting heaving rates. 3rd International Conference on Permafrost, 722–728, Edmonton, Alberta, Canada.
Richards, L.A., 1931. Capillary conduction of liquids through porous mediums. Physics 1, 318–333.
Shao, M., Wang, Q., Huang, M., 2006. Soil Physics. Higher Education Press, Beijing, China pp. 90–94 (in Chinese).
Spaans, E.J.A., Baker, J.M., 1996. The soil freezing characteristic: its measurement and similarity to the soil moisture characteristic. Soil Sci. Soc. Am. J. 60 (1), 13–19.
Taylor, G.S., Luthin, J.N., 1978. A model for coupled heat and moisture transfer during soil freezing. Can. Geotech. J. 15 (4), 548–555.
Wettlaufer, J.S., Worster, M.G., 1995. Dynamics of premelted films: frost heave in a capillary. Phys. Rev. E. 51 (5), 4679–4689.
Wettlaufer, J.S., Worster, M.G., Wilen, L.A., et al., 1996. A theory of premelting dynamics for all power law forces. Phys. Rev. Lett. 76 (15), 3602–3605.
Xu, X., Deng, Y., 1991. Experimental Study on Water Migration in Freezing and Frozen Soil. Science Press, Beijing, China pp. 36–45 (in Chinese).
Xu, X., Zhang, L., Deng, Y., et al., 1993. Unfrozen water content in multi-crystal ice. J. Glaciol. Geocryol. 15 (1), 149–152 (in Chinese).

Xu, X., Wang, J., Zhang, L., 2010. Frozen Soil Physics. Science Press, Beijing, China pp. 86–89 (in Chinese).
Zhou, Y., Zhou, G., 2010. Finite volume simulation for coupled moisture and heat transfer during soil freezing. Chin. J. Geotech. Eng. 32 (3), 440–446 (in Chinese with English abstract).
Zhou, J., Li, D., Fang, J., et al., 2011. Numerical analysis of heat and mass transfer in saturated freezing soil in an open system. J. Glaciol. Geocryol. 32 (4), 791–795 (in Chinese with English abstract).
Zimmerman, W.B.J., 2007. COMSOL Multiphysics-FEM multiphysics modeling and analysis. China Communications Press, Beijing, China pp. 153–157 (in Chinese).